

Reconstruction of Two-Dimensional Permittivity Distribution Using the Distorted Born Iterative Method

W. C. CHEW AND Y. M. WANG

Abstract—The distorted Born iterative method (DBIM) is used to solve two-dimensional inverse scattering problems. The purpose of this algorithm is to provide another general method to solve the two-dimensional imaging problem when the Born and the Rytov approximations break down. Numerical simulations are performed using the distorted Born iterative method and the method proposed in our previous paper [called the Born iterative method (BIM)] for several cases where the conditions for the first-order Born approximation are not satisfied. The results show that each method has its advantages. The distorted Born iterative method shows faster convergence rate compared to the Born iterative method, while the Born iterative method is more robust to noise contamination compared to the distorted Born iterative method.

I. INTRODUCTION

IN our previous paper [1], we proposed a Born iterative method (BIM) where the Green's function remains unchanged in the iterative procedures for solving the two-dimensional electromagnetic inverse scattering problem when the first Born approximation breaks down. Here, an alternative procedure called the distorted Born iterative method (DBIM), where the Green's function is updated in every iteration step, is proposed for solving the same problem.

Although intensive research has been performed on the linear diffraction tomography for more than a decade [2]–[8], [11], few works have been reported on the more general and important higher-dimensional, nonlinear inverse scattering problem [12], [16], [17]. The distorted Born iterative method has been used to solve the one-dimensional inverse scattering problem [9], [10]. In the present paper, we first present the formulation of the method in Section II. In Section III, the numerical simulations will be given using both methods: the distorted Born iterative method, and the Born iterative method [1]. Numerical results show that the distorted Born iterative method converges faster than the Born iterative method, while the

Born iterative method is more tolerant to noise than the distorted Born iterative method. Depending on the problem to be solved, both of them are competing candidates for solving the inverse scattering problem beyond the Born approximation.

II. FORMULATION

The geometry of the two-dimensional inverse problem is shown in Fig. 1. The cylindrical medium with an arbitrary cross section is inhomogeneous in the xy plane but is homogeneous in z direction. The receivers are located around the cylindrical object at finite discrete points. The object is illuminated by either a plane wave or a field excited by a line source indicated as T in Fig. 1. A scalar wave equation $(\nabla^2 + k^2)\phi(x, y) = 0$ will be used to describe the field. This represents an acoustic wave. In the electromagnetic case, it is a TM (transverse magnetic) to z wave. For a TM incident wave, the corresponding integral equation is

$$E_z(x, y) = E_z^i(x, y) + \iint_S G(\boldsymbol{\rho} - \boldsymbol{\rho}', \epsilon_r^b) \cdot k_0^2 \delta\epsilon_r E_z(x', y') dx' dy', \quad (1)$$

where S is the scatterer cross section, and $G(\boldsymbol{\rho} - \boldsymbol{\rho}', \epsilon_r^b)$ is the solution of following equation:

$$\nabla_s^2 G(\boldsymbol{\rho} - \boldsymbol{\rho}', \epsilon_r^b) + k_b^2(x, y) G(\boldsymbol{\rho} - \boldsymbol{\rho}', \epsilon_r^b) = -\delta(\boldsymbol{\rho} - \boldsymbol{\rho}'). \quad (2)$$

Here,

$$\nabla_s^2 \equiv \frac{\partial^2}{\partial x^2} + \frac{\partial^2}{\partial y^2},$$

$$k_b^2 = k_0^2 \epsilon_r^b(x, y),$$

and ϵ_r^b is the background relative permittivity. For homogeneous ϵ_r^b , $G(\boldsymbol{\rho} - \boldsymbol{\rho}', \epsilon_r^b)$ in a closed form is

$$G(\boldsymbol{\rho} - \boldsymbol{\rho}') = \frac{i}{4} H_0^{(1)}(k_0 |\boldsymbol{\rho} - \boldsymbol{\rho}'|). \quad (3)$$

For an inhomogeneous background $\epsilon_r^b(x, y)$, $G(\boldsymbol{\rho} - \boldsymbol{\rho}', \epsilon_r^b)$ has to be solved numerically.

Manuscript received June 28, 1989; revised November 30, 1989. This work was supported by the National Science Foundation under Grant NSF ECS-85-25891, by the Office of Naval Research under Grant N000-14-89-J1286, by Schlumberger, and by TRW. Computer time was partly provided by the National Center for Supercomputer Applications at the University of Illinois.

The authors are with the Electromagnetics Laboratory, Department of Electrical and Computer Engineering, University of Illinois, Urbana, IL 61801.

IEEE Log Number 9034446.

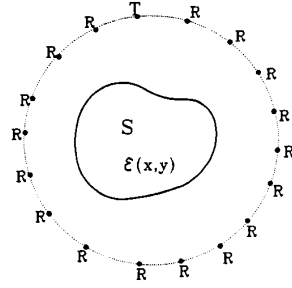


Fig. 1. Geometrical configuration of the problem.

In solving the inverse scattering problem, the measurements are performed around the scatterer at R indicated in Fig. 1. The integral equation (1) then becomes

$$E_z^s(x, y) = \iint_S G(\boldsymbol{\rho} - \boldsymbol{\rho}', \epsilon_r^b) k_0^2 \epsilon_r E_z(x', y') dx' dy', \quad (4)$$

and

$$\delta\epsilon_r = \epsilon_r(x, y) - \epsilon_r^b(x, y) \quad (5)$$

is the permittivity profile to be reconstructed. In the iterative procedure proposed in our previous paper [1], the Green's function remains unchanged throughout the iteration, implying that ϵ_r^b in the above equation is constant, which is the free-space relative permittivity. We call this the Born iterative method because, in each iteration, the kernel of the integral operator remains unchanged, only the field in the scatterer is updated. One immediate extension of this method is to update the Green's function, the kernel of integration, as well as the field in the scatterer. By updating the Green's function, extra computational effort is needed to calculate the point-source response in the scatterer for every observation point. Fortunately, when the inverse of the matrix is known from solving the forward problem, the extra computational effort for the point-source response in the scatterer is proportional to MN^2 , where M is the number of the measurements and N is the number of unknowns modeling the scatterer. For most practical situations, the number of unknowns is much larger than the number of measurements, i.e., $N \gg M$. Therefore, the extra computational effort needed to calculate the Green's function is of an order smaller than that for solving the forward problem at each iteration step. The salient features of the new iterative procedure for solving the nonlinear integral equation (4) is briefly sketched as follows.

1) Solve the linearized inverse problem for the first-order object function by using the Born approximation where the homogeneous Green's function of (3) with the unit relative permittivity is used.

2) Solve the forward scattering problem using the method of moments [18], [19] for the field in the object and at the observation points. Next, calculate the point-source response in the object for every observation point

with the last reconstructed object function. The second part of this step is to calculate the Green's function with the last reconstructed permittivity distribution as the background permittivity $\epsilon_r^b(x, y)$.

3) Substitute the new Green's function and the field obtained in step 2) into the integrand, and subtract the scattered field at the receivers from the left-hand side of integral equation (4). Then solve the above inverse problem for the corrections to the last reconstructed profile. Generate the new profile by adding the corrections to the previous profile.

4) Repeat step 2) and compare the field scattered by the reconstructed distribution function and the measured data which, in our case, are the simulated fields for the exact distribution function at the receiver points. If the relative residual error (RRE) (see definition below) is less than a criterion which was given before or is larger than the RRE of the last reconstructed profile, the iteration terminates. Otherwise, repeat the cycle until the solution converges.

The definition of the relative residual error (RRE) in the j th iteration is

$$\text{RRE} = \frac{\sum_{i=1}^M |E_z^s(\boldsymbol{\rho}_i) - E_z^{s(j)}(\boldsymbol{\rho}_i)|}{\sum_{i=1}^M |E_z^s(\boldsymbol{\rho}_i)|} \quad (6)$$

where the summation is over the receiver points.

A. Direct Scattering Solution and the Green's Function

To implement the above procedure on a computer, both the forward [step 2) and step 4)] and the inverse [step 1) and step 3)] problems need to be discretized. For consistency, we choose the same basis function $f_i(x, y)$ for both of them. For simplicity and comparison with the Born iterative method we proposed in our previous paper, the pulse basis function $f_i(x, y)$ has been used in discretizing both the direct and the inverse scattering problems. The point-matching method [18], [19] is employed in solving the forward scattering problem and in calculating the Green's function with the permittivity distribution at every iteration step.

The field and the permittivity of the object are represented as

$$E_z(x, y) = \sum_{i=1}^N e_i f_i(x, y), \quad (7)$$

$$\delta\epsilon_r(x, y) = \sum_{i=1}^N a_i f_i(x, y). \quad (8)$$

The equation of the forward scattering problem can be written as

$$\bar{\Gamma} \cdot \mathbf{e} = \mathbf{b}, \quad (9)$$

where \mathbf{e} is an unknown column vector whose entries are the expansion coefficients of $E_z(x, y)$ expressed in (7), and \mathbf{b} is the expansion coefficients of the incident field in

the first term on the right-hand side of (1). The elements of matrix Γ are

$$\Gamma_{ij} = \delta_{ij} - \iint_{S_i} G_0(\boldsymbol{\rho} - \boldsymbol{\rho}') k_0^2 \delta \epsilon_r \delta(x' - x_i) \cdot \delta(y' - y_i) f_i(x, y) dx' dy' dx dy. \quad (10)$$

The linear system of equations for calculating the Green's function is the same as (9), except that the entries in the column vector \mathbf{b} comprise the incident field generated by a two-dimensional point source located at the corresponding receiver point.

It is worthy to note that to calculate the Green's function numerically in every iterative step, the matrix inverse model is exactly that for solving the forward scattering problem. Therefore, if the matrix has been inverted in solving the forward scattering problem, the same matrix inverse is directly applied to calculate the Green's function so that the extra computational effort is proportional to MN^2 , where M is the number of receivers and N is the number of basis functions used in the discretization of the problem. In most practical situations, the number of unknowns is much larger than that of receivers, i.e., $N \gg M$. Therefore, compared to the computational time spent on solving the forward problem, which is proportional to N^3 , the extra time spent on the calculation of the Green's function in each iterative step is not that significant.

B. Inverse Scattering Solution

For a linearized version of the integral equation (1), the linear system of equations for the inverse scattering problem is

$$E_z^{s(l)}(x_j, y_j) = \sum_{i=1}^N a_i^{(l+1)} \iint_{S_i} G_l(\boldsymbol{\rho}_j - \boldsymbol{\rho}', \epsilon_r^l) \cdot k_0^2 f_i(x', y') E_z^{(l)}(x', y') dx' dy' \quad j = 1, \dots, M' \quad (11)$$

where S_i is the domain of the pulse function $f_i(x, y)$, and $E_z^{(l)}$ is the l th forward scattering solution with the l th permittivity distribution function. For $l = 0$, it is the incident field in the object, and (8) has been used to express $\delta \epsilon_r$ in terms of the basis function $f_i(x, y)$. $G_l(\boldsymbol{\rho}_j - \boldsymbol{\rho}', \epsilon_r^l)$ is the Green's function with the permittivity distribution ϵ_r^l which has been obtained numerically.

Equation (11) for the inverse scattering problem can be written as the matrix equation

$$\mathbf{b} = \bar{\mathbf{K}} \cdot \mathbf{a} \quad (12)$$

where

$$\mathbf{b} = (E_z^s(\boldsymbol{\rho}_1), E_z^s(\boldsymbol{\rho}_2), \dots, E_z^s(\boldsymbol{\rho}_M))^T, \\ \mathbf{a} = (a_1, a_2, \dots, a_N)^T,$$

and $\bar{\mathbf{K}}$ is an $M \times M$ matrix whose elements are

$$K_{ji} = \iint_{S_i} k_0^2 G_l(\boldsymbol{\rho}_j - \boldsymbol{\rho}', \epsilon_r^l) E_z^{(l)}(x', y') \cdot f_i(x', y') dx' dy' \\ i = 1, \dots, N, \quad j = 1, \dots, M.$$

It is well known that (12) of the inverse scattering problem is ill posed [14]–[16]. In order to find an adequate solution of (12), the regularization procedure [20], [21] is employed to circumvent the instability of the problem. In the regularization procedure, instead of solving the matrix equation (12) directly for a least-square solution, we can solve an optimization problem which minimizes the cost function $C(\mathbf{a})$, defined as

$$C(\mathbf{a}) = \|\bar{\mathbf{K}} \cdot \mathbf{a} - \mathbf{b}\|^2 + \gamma \|\bar{\mathbf{H}} \cdot \mathbf{a}\|^2, \quad (13)$$

where γ is the regularization parameter, and $\bar{\mathbf{H}}$ is the smoothing matrix. From (13), one obtains the following matrix equation:

$$[\bar{\mathbf{K}}^\dagger \cdot \bar{\mathbf{K}} + \gamma \bar{\mathbf{H}}^\dagger \cdot \bar{\mathbf{H}}] \cdot \mathbf{a} = \bar{\mathbf{K}}^\dagger \cdot \mathbf{b}, \quad (14)$$

where $\bar{\mathbf{K}}^\dagger$ and $\bar{\mathbf{H}}^\dagger$ are the conjugate transpose of $\bar{\mathbf{K}}$ and $\bar{\mathbf{H}}$, respectively. In this paper, the zeroth-order regularization, in which $\bar{\mathbf{H}}$ is the identity matrix of order N , has been used to generate results given in the next section. A solution of (14) is given by

$$\mathbf{a} = [\bar{\mathbf{K}}^\dagger \cdot \bar{\mathbf{K}} + \gamma \bar{\mathbf{K}}^\dagger \cdot \bar{\mathbf{K}}]^{-1} \cdot \bar{\mathbf{K}}^\dagger \cdot \mathbf{b}. \quad (15)$$

More attention is needed to choose an adequate regularization parameter γ in solving the above equation.

III. NUMERICAL RESULTS

Before presenting some numerical results, we define and review some terminologies which will be used in the following numerical analysis. First, we define the relative Mean Square Error (MSE) of the reconstructed permittivity profile as

$$\text{MSE} = \sqrt{\frac{\iint_S [\epsilon_r^{(i)}(\boldsymbol{\rho}) - \epsilon_r(\boldsymbol{\rho})]^2 dx dy}{\iint_S [\epsilon_r(\boldsymbol{\rho})]^2 dx dy}} \quad (16)$$

where S is the scatterer's cross section, $\epsilon_r^{(i)}(\boldsymbol{\rho})$ is the reconstructed relative permittivity distribution in the i th iteration, and $\epsilon_r(\boldsymbol{\rho})$ is the original relative permittivity distribution. In actual application, MSE is unknown since $\epsilon_r(\boldsymbol{\rho})$ is not known. Second, the Relative Residual Error of j th iterative reconstructed permittivity profile is defined in (6).

As the first example, Fig. 2 shows clearly the evolution of the convergence of the solution given by the distorted Born iterative algorithm for an asymmetric permittivity distribution. Fig. 2(a) is the original dielectric distribution. Fig. 2(b) is the first-order Born approximation. Fig. 2(c)–(h) shows the iterative results from the second iter-

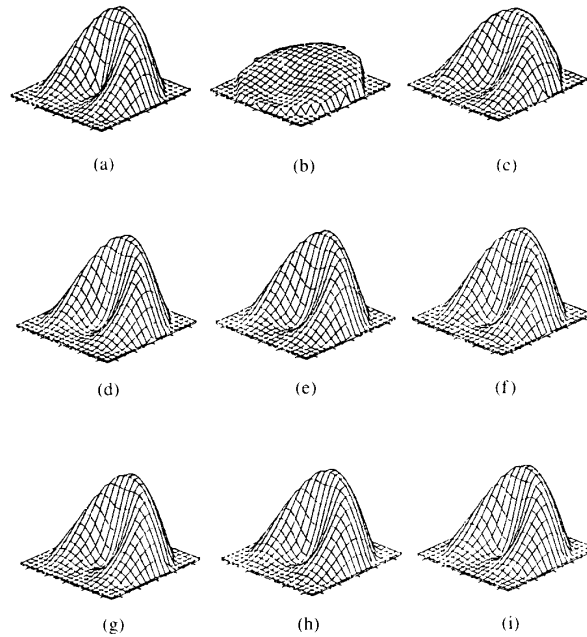


Fig. 2. Reconstruction of an asymmetric distribution with operating frequency at 100 MHz. The peak value of the relativity permittivity is 1.8. The diameter of the object is one wavelength. (a) is the original distribution. (b) is the result of the first-order approximation. (c)-(h) are the results from the second iteration to the seventh iteration. (i) is the final convergent solution after 25 iterations.

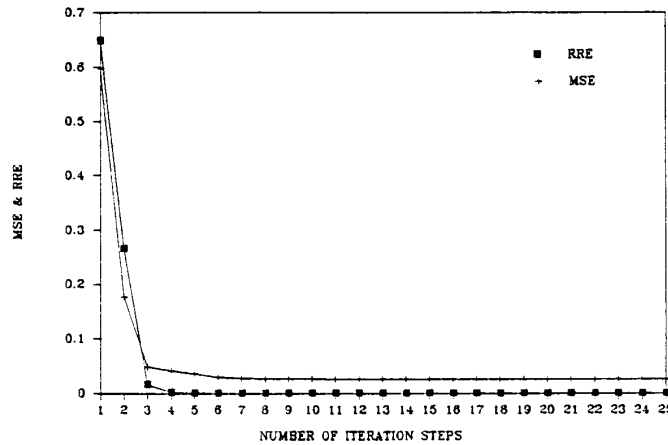


Fig. 3. The relative MSE (Mean Squared Error) and the RRE (Relative Residual Error) of the reconstructed permittivity distribution in Fig. 2 as a function of the iteration steps.

ation to the seventh iteration. Fig. 2(i) gives the final convergent solution after 25 iterations. Actually, it is hard to tell the difference between (e) and (i). The reason why the algorithm terminates after the 25th iteration is that we have chosen a relatively small RRE as a convergent criterion in this case (10^{-5}) to examine the convergence and the stability of the algorithm.

Fig. 3 shows the relative mean square error (MSE) and relative residual error (RRE) of the reconstructed permit-

tivity distribution in the last example as a function of the iteration steps. It is clear that the RRE drops to a negligible level after the fourth iteration. The MSE stays at 0.026 after the sixth iteration because of the band-limited effect of the algorithm. For example, a discontinuity at the origin of the original permittivity distribution is smoothed out in the reconstruction.

This example gives us an idea on how the algorithm proposed in the present paper works for a general permit-

tivity reconstruction problem for asymmetric and non-smooth distribution.

In the following examples, both the results of the distorted Born iterative method and the Born iterative method are given for comparison for every case.

A. Sin-Like Distribution (Noiseless)

Fig. 4 shows the reconstruction of a sin-like permittivity distribution by using the distorted Born iterative method. The diameter of the object is about 1λ . Fig. 4(a) is the original distribution. Fig. 4(b) is the result of the first-order Born approximation. Fig. 4(c)–(e) shows the iterative solution from the second step to the fourth step. Fig. 4(f) gives the convergent solution after the 15 iterations.

Fig. 5 shows the reconstruction of the same distribution by using the Born iterative method. The meaning of the curve surfaces are the same as that in Fig. 4.

Fig. 6 shows the relative mean square error and the relative residual error as a function of the iterative steps for both the distorted Born and the Born iterative methods. It shows that for the distorted Born iterative method, the convergent solution is achieved after the fourth iteration, while for the Born iterative method, the convergent solution is reached after the sixth iteration.

B. Two Separated Pulses (Noiseless)

Fig. 7 shows the reconstruction of the two pulse distribution using the distorted Born iterative method. The dimension of the pulses is about $\lambda/4$. The distance between the two pulses is about $\lambda/4$. Fig. 7(a) is the original distribution. Fig. 7(b) is the reconstructed distribution of the first-order Born approximation. Fig. 7(c)–(h) shows the reconstructed distributions from the second to the seventh iterations. Fig. 7(i) is the result after 15 iterations.

Fig. 8 shows the reconstruction of the same distribution by using the Born iterative method.

Fig. 9 gives the relative residual error (RRE) of the reconstructed distributions as a function of the iteration steps for both the distorted Born and Born iterative methods. The difference at step 1 is due to the different choices of regularization parameters in (14) for both cases.

From this example, we see that both methods successfully distinguish the two pulses from each other. However, the convergent speed of the Born iterative method seems much slower than that of the distorted Born iterative method.

Up to now, all the examples given in this paper are noise free. To achieve the same accuracy for the reconstructed solution, the Born iterative method needs at least two more iteration steps than the distorted Born iterative method.

C. Sin-Like Distribution with Noise

Fig. 10 shows the reconstruction of a sin-like permittivity distribution with 25 dB of the signal-to-noise ratio by using the distorted Born iterative method. The diam-

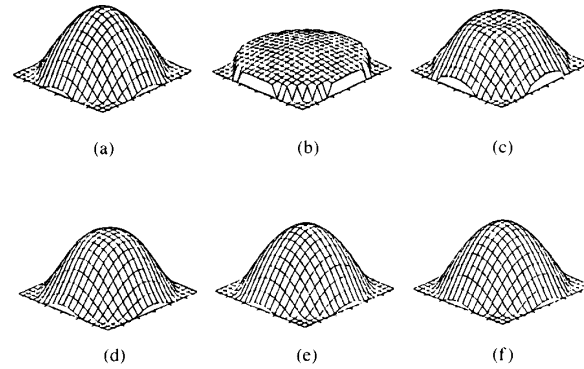


Fig. 4. Reconstruction of a sin-like permittivity distribution by using the distorted Born iterative method with operating frequency at 100 MHz. The peak value of the relative permittivity is 1.8. The diameter of the object is 1λ . (a) is the original distribution. (b) is the result of the first-order approximation. (c)–(e) are the results from the second iteration to the fourth iteration. (f) is the final convergent solution after 15 iterations.

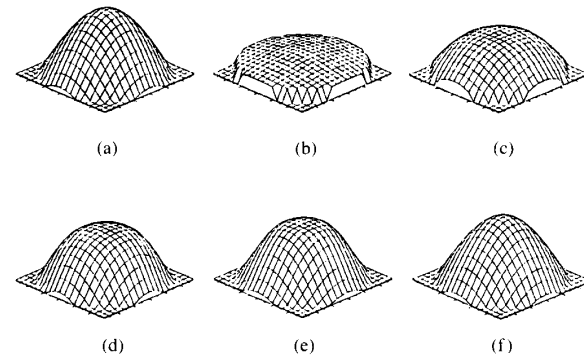


Fig. 5. Reconstruction of a sin-like permittivity distribution by using the Born iterative method with operating frequency at 100 MHz. The peak value of the relative permittivity is 1.8. The diameter of the object is 1λ . (a) is the original distribution. (b) is the result of the first-order approximation. (c)–(e) are the results from the second iteration to the fourth iteration. (f) is the final convergent solution after 15 iterations.

eter of the object is 1λ . The peak value of the sin-like distribution is 1.8. Fig. 10(a) is the reconstructed distribution of the first-order Born approximation. Fig. 10(b)–(e) shows the iterative results from the second to fifth iterations. Fig. 10(f) is the result after a filtering operation which we shall describe later. The algorithm terminates after five iterations because the relative residual error in the fifth iteration is larger than the RRE in the fourth iteration (see Fig. 12 below). The plot of the original permittivity distribution is given in Fig. 11(a).

Fig. 11 shows the reconstruction of the same problem given in the above by using the Born iterative method. Fig. 11(a) is the original distribution. Fig. 11(b) is the reconstruction of the first-order Born approximation. Fig. 11(c)–(g) shows the results from the second iteration to the sixth iteration. Fig. 11(h) is the final result after 15 iterations. Here we have set the maximum number of steps as 15. Fig. 11(i) is the filtered result.

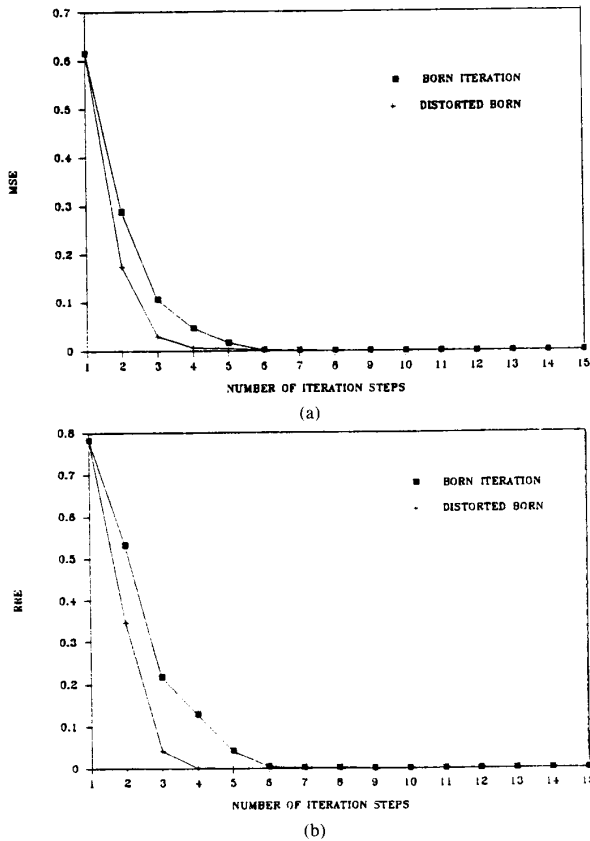


Fig. 6. (a) is the relative MSE (Mean Squared Error) of the reconstructed permittivity distributions in Figs. 4 and 5 as a function of the iteration steps. (b) is the RRE (Relative Residual Error) of the reconstructed permittivity distributions as a function of the iteration steps.

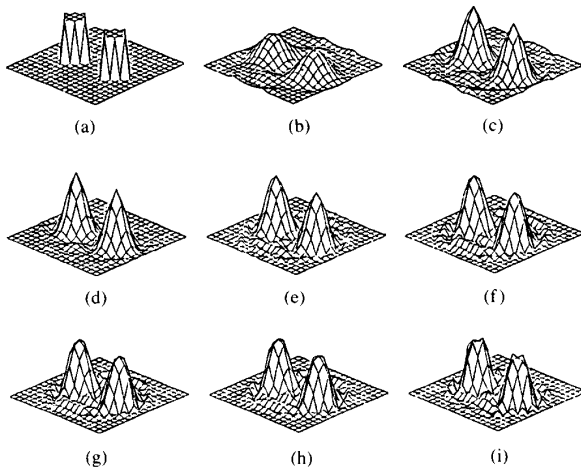


Fig. 7. Reconstruction of a two-pulse distribution by using the distorted Born iterative method with the operating frequency at 100 MHz. The peak value of the relative permittivity is 1.8. The dimension of the pulses is about $\lambda/4$. The distance between the two pulses is about $\lambda/4$. (a) is the original distribution. (b) is the result of the first-order approximation. (c)-(h) are the results from the second iteration to the seventh iteration. (i) is the final convergent solution after 15 iterations.

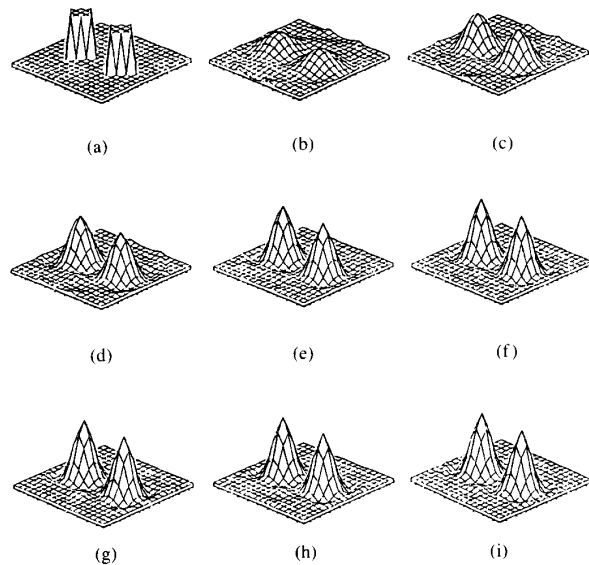


Fig. 8. Reconstruction of a two-pulse distribution by using the Born iterative method with the operating frequency at 100 MHz. The peak value of the relative permittivity is 1.8. The dimension of the pulses is about $\lambda/4$. The distance between the two pulses is about $\lambda/4$. (a) is the original distribution. (b) is the result of the first-order approximation. (c)-(h) are the results from the second iteration to the seventh iteration. (i) is the final convergent solution after 15 iterations.

Fig. 12 gives the MSE and the RRE as a function of iteration steps for both the distorted Born and the Born iterative methods. As we see, the MSE of the distorted Born iterative method increases at the fifth iteration step. This is consistent with Fig. 10(e) which is noisier than that of Fig. 10(d). Fortunately, at the same step, the RRE increases as well [see Fig. 12(b)] so that the program is terminated after this step. However, the convergent behavior of the Born iterative method is quite different. Both the RRE and MSE reach the final convergent solution after a few steps, and both of them stay at that value until the program terminates after the iteration reaches the maximum iteration steps.

When noise exists, unwanted artifacts are present in the reconstructed distribution, which could be easily recognized in Fig. 10(e) and Fig. 11(h). This image noise obscures the actual object features. For this reason, image filters are used to remove the noise so that the features can be identified [22]. The filter operates by passing a 5-cell window over the image, and replacing the center cell of the window with some function of all the cells in the window. One obvious function would be one that averages all the cells in the window. Unfortunately, this type of filter is too harsh because in addition to removing the noise in the image, it also blurs the desired features of the distribution function of the object. In this paper, the weighted average filter of all the cells in the window has been chosen in which weighting factors are chosen as 1.8 for the center cell and 0.8 for the other cells. Fig. 10(f) and Fig. 11(i) are the final reconstructed distributions after filtering on Fig. 10(d) and Fig. 11(e), respec-

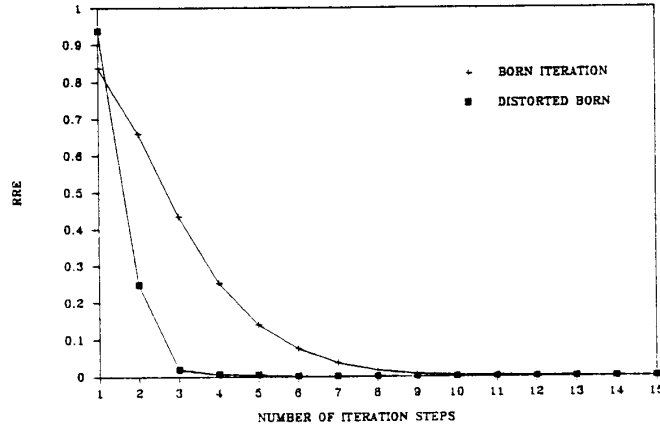


Fig. 9. The RRE (Relative Residual Error) of the reconstructed permittivity distribution in Figs. 7 and 8 as a function of the iteration steps.

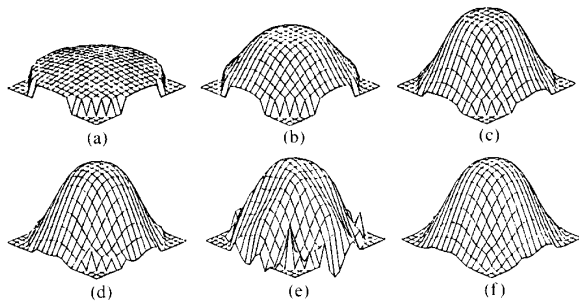
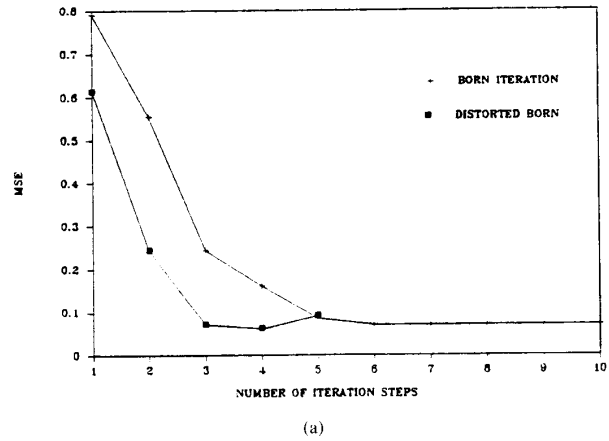


Fig. 10. Reconstruction of a sin-like permittivity distribution with a 25 dB signal-to-noise ratio in the measurement field by using the distorted Born iterative method with operating frequency at 100 MHz. The peak value of the relativity permittivity is 1.8. The diameter of the object is 1λ . (a) is the original distribution. (b) is the result of the first-order approximation. (c)–(e) are the results from the second iteration to the fourth iteration. (f) is the final distribution after operating the filter function on (d).



(a)

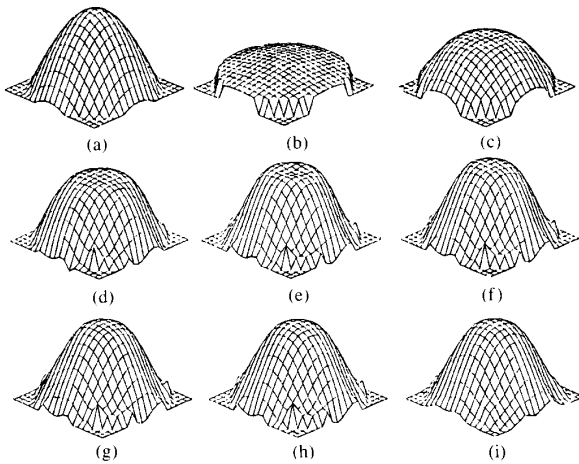
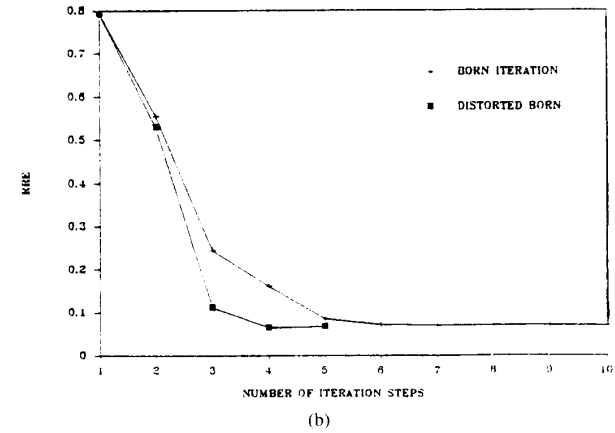


Fig. 11. Reconstruction by using the Born iterative method for the same problem given in Fig. 10. (a) is the original distribution. (b) is the result of the first-order approximation. (c)–(g) are the results from the second iteration to the sixth iteration. (h) is the convergent distribution after the 15 iterations. (i) is the reconstructed distribution after operating the filter function on (h).



(b)

Fig. 12. (a) is the relative MSE (Mean Squared Error) of the reconstructed permittivity distributions in Figs. 10 and 11 as a function of the iteration steps. (b) is the RRE (Relative Residual Error) of the reconstructed permittivity distributions in Figs. 10 and 11 as a function of the iteration steps.

tively. The reason for using Fig. 10(d) instead of Fig. 10(e) is that both of the MSE and the RRE at step four are smaller than that at step five, such that it is more reliable to use Fig. 10(d) instead of Fig. 10(e).

D. Discussions

In the above, we give the examples using both the distorted Born iterative and the Born iterative methods to reconstruct the permittivity profiles. In the noiseless cases, the distorted Born iterative method displays faster convergence than the Born iterative method. However, for the noisy cases, the Born iterative method is more robust than the distorted Born iterative method. The example given in this paper with the noisy case for the distorted Born iterative method is acceptable because the program is terminated immediately just after the MSE increases. However, if the MSE and the RRE do not increase at the same step, the final reconstructed profile could be quite noisy. The reason why the distorted Born iterative method is more susceptible to noise contamination is explained in the following paragraph.

The left-hand side of (4) is unchanged in the iterative process for the Born iterative method which is the scattered field by the object with the free-space background. However, for the distorted Born iterative method, the left-hand side of (4) has to be subtracted from the scattered field of the last iterative reconstructed distribution with the background as the distribution before the last iteration. If the noise is added in the scattered field at the beginning (in our case, 25 dB signal-to-noise ratio, which is equivalent to about 5.6% random noise, has been added in the examples given in Fig. 10 and 11), then after a few iterations, the noise will dominate the left-hand side of (4). Consequently, the correction of the distribution after that step only contributes to the noise of the constructed distribution and no more information of the object could be derived.

IV. CONCLUSION

An alternative iterative method, called the distorted Born iterative method, has been presented for solving the two-dimensional nonlinear inverse scattering problem. The comparison has been made between this method and the method proposed in our previous paper. The results show that for the noiseless cases, the distorted Born iterative method is superior to the Born iterative method because of its faster convergent speed, while for the noisy cases, the Born iterative method is more robust than the distorted Born iterative method. The simulation is limited to the objects of two wavelengths or less because of the available computational resources. Larger problems can be studied with such algorithm. The size of the object

may or may not affect the validity of the algorithm, and should be a topic of further research.

REFERENCES

- [1] Y. M. Wang and W. C. Chew, "An iterative solution of two-dimensional electromagnetic inverse scattering problem," *Int. J. Imaging Syst. Technol.*, vol. 1, no. 1, pp. 100-108, 1989.
- [2] A. J. Devaney, "A computer simulation of diffraction tomography," *IEEE Trans. Biomed. Eng.*, vol. BME-30, pp. 377-386, 1983.
- [3] M. Azimi and A. C. Kak, "Distortion in diffraction tomography caused by multiple scattering," *IEEE Trans. Med. Imaging*, vol. MI-2, pp. 176-195, 1983.
- [4] W. Tabbara, B. Duchêne, Ch. Pichot, D. Lesselier, L. Chommeloux, and N. Joachimowicz, "Diffraction tomography: Contribution to the analysis of applications in microwaves and ultrasonics," *Inverse Problem*, vol. 4, pp. 305-331, 1988.
- [5] A. J. Devaney, "A filtered backpropagation algorithm for diffraction tomography," *Ultrasonic Imaging*, vol. 4, pp. 336-360, 1982.
- [6] J. B. Keller, "Accuracy and validity of the Born and Rytov approximations," *J. Opt. Soc. Amer.*, vol. 59, pp. 1003-1004, 1969.
- [7] M. Slaney, A. C. Kak, and L. E. Larsen, "Limitations of imaging with first-order diffraction tomography," *IEEE Trans. Microwave Theory Tech.*, vol. MTT-32, pp. 860-874, 1984.
- [8] E. Wolf, "Three-dimensional structure determination of semi-transparent objects from holographic data," *Opt. Commun.*, vol. 1, pp. 153-169, 1969.
- [9] W. C. Chew and S. L. Chuang, "Profile inversion of a planar medium with a line source or a point source," in *Proc. Int. Geosci. Remote Sensing Symp.*, Inst. Elec. Electron. Eng., Strasbourg, France, 1984.
- [10] T. M. Habashy, W. C. Chew, and E. Y. Chow, "Simultaneous reconstruction of permittivity and conductivity profiles in a radially inhomogeneous slab," *Radio Sci.*, vol. 21, no. 4, pp. 635-645, 1986.
- [11] D. K. Ghodgonkar, O. P. Gandhi, and M. J. Hagmann, "Estimation of complex permittivities of three-dimensional inhomogeneous biological bodies," *IEEE Trans. Microwave Theory Tech.*, vol. MTT-31, pp. 442-446, June 1983.
- [12] M. M. Ney, A. M. Smith, and S. S. Stuchly, "A solution of electromagnetic imaging using pseudoinverse transformation," *IEEE Trans. Med. Imaging*, vol. MI-3, pp. 155-162, Dec. 1984.
- [13] N. Bleistein and J. K. Cohen, "Nonuniqueness in the inverse source problem in acoustics and electromagnetics," *J. Math. Phys.*, vol. 18, pp. 194-201, Feb. 1977.
- [14] A. J. Devaney and G. C. Sherman, "Nonuniqueness in inverse source and scattering problems," *IEEE Trans. Antennas Propagat.*, vol. 30, pp. 1034-1042, Sept. 1982.
- [15] A. J. Devaney and E. Wolf, "Radiating and nonradiating classical current distributions and the fields they generate," *Phys. Rev. D*, vol. 8, pp. 1044-1047, Aug. 1973.
- [16] S. J. Johnston and M. L. Tracy, "Inverse scattering solutions by a sine basis, multiple source, moment method—Part I: Theory," *Ultrasonic Imaging*, vol. 5, pp. 361-375, 1983.
- [17] —, "Inverse scattering solutions by a sine basis, multiple source, moment method—Part II: Numerical evaluations," *Ultrasonic Imaging*, vol. 5, pp. 376-392, 1983.
- [18] J. Richmond, "Scattering by a dielectric cylinder of arbitrary cross-sectional shape," *IEEE Trans. Antennas Propagat.*, vol. AP-13, pp. 334-341, 1965.
- [19] R. F. Harrington, *Field Computation by Moment Methods*. Malabar, FL: Krieger, 1983.
- [20] S. Twomey, *Introduction to the Mathematics of Inversion in Remote Sensing and Indirect Measurements*. New York: Elsevier Scientific, 1977.
- [21] C. T. H. Baker, *The Numerical Treatment of Integral Equations*. Oxford: Clarendon, 1977.
- [22] M. Frank and C. A. Balanis, "Method for improving the stability of electromagnetic geophysical inversions," *IEEE Trans. Geosci. Remote Sensing*, vol. 27, pp. 339-343, May 1989.